Electronic Supplementary Material (ESI) for Chemical Communications.

Nanoparticle-electrode collisions as a dynamic seeding route for the growth of anisotropic metallic nanostructures

Andrew Pearson[a] and Anthony P. O'Mullane[b,*]

[a] School of Applied Sciences, RMIT University, GPO Box 2476V, Melbourne, Australia.

[b] School of Chemistry, Physics and Mechanical Engineering, Queensland University of Technology, GPO Box 2434, Brisbane, QLD 4001, Australia.

*Email: anthony.omullane@qut.edu.au.

Supplementary Information

Experimental

Silver nitrate ($AgNO_3$), chloroauric acid ($HAuCl_4$), tyrosine, tri-sodium citrate, sodium hydroxide ($NaOH$), lead (II) nitrate ($Pb(NO_3)_2$), hydrochloric acid (HCl) and hydrazine were obtained from Sigma-Aldrich and were used as-received.

Ag-tyrosine nanoparticles (TEM image shown in Fig. S1A) were synthesised by adding 18 mg tyrosine (final concentration of 1 mM) and 1 mL of 0.1 M NaOH to a boiling solution of 1 mM $AgNO_3$ in 100 mL of deionised (MilliQ) water under rapid stirring, the solution was observed to turn bright yellow in colour over a period of 5 minutes. After 30 minutes the solution was allowed to cool and used in subsequent experiments without further modification. Au-citrate nanoparticles (TEM image shown in Fig. S1B) were synthesised by first boiling 100 mL of a rapidly stirred 1 mM $HAuCl_4$ solution. To this solution 7 mL of a 5% aqueous tri-sodium citrate solution was added after which the solution turned wine red in colour over a period of 10 minutes after which the solution was allowed to cool and was employed in subsequent experiments without further modification.

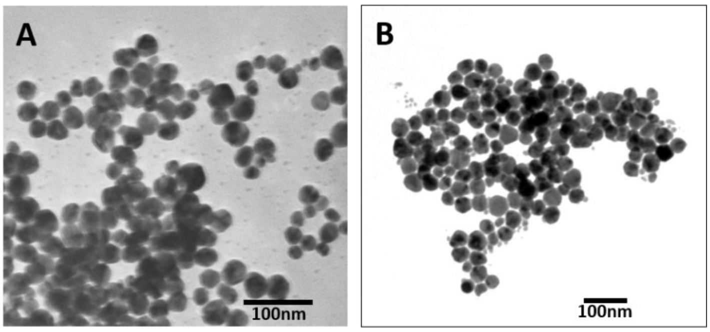

Figure S1: TEM images of (A) Ag-tyr NPs and (B) Au-cit NPs.

Plating solutions for the deposition of Ag and Au nanostructures were consisted of 5 mL of 1 mM $AgNO_3$ or $HAuCl_4$ containing 0, 50 µM, 500 µM or 1 mM Ag-tyr or Au-cit nanoparticles. Ag and Au nanostructures were formed electrochemically using a CH instruments (CHI760C) electrochemical analyser (Ag/AgCl (3M KCl) reference and platinum wire counter electrodes respectively) by applying a potential of -100 mV (300 mV for Au) for 300 seconds on a 5 mM diameter circular glassy carbon substrate after which the substrates were removed from the plating solution and washed three times with deionised water. Scanning Electron Microscopy was performed on an FEI Nova NanoSEM at an operating voltage of 15 kV under high-vacuum conditions.

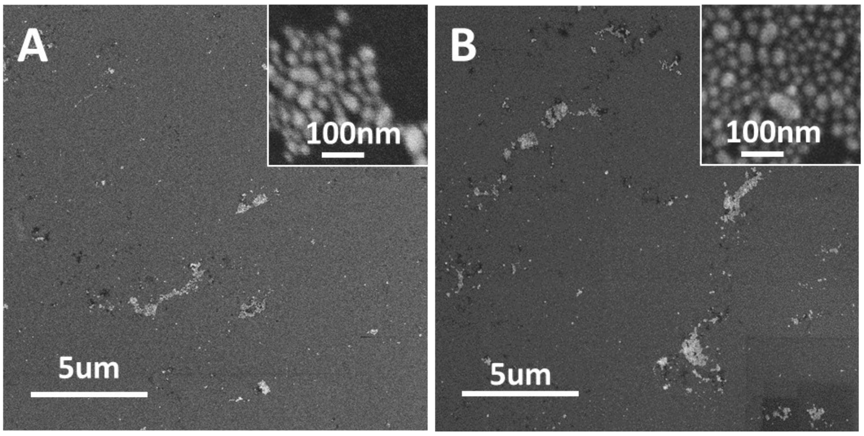

Figure S2: Scanning Electron Microscope images of Ag-tyr nanoparticles (A) and Au-cit nanoparticles (B) adhered to the glassy carbon electrode surface after application of -100 mV potential (for Ag-tyr) and 300 mV potential (Au-cit) for a period of 300 seconds.

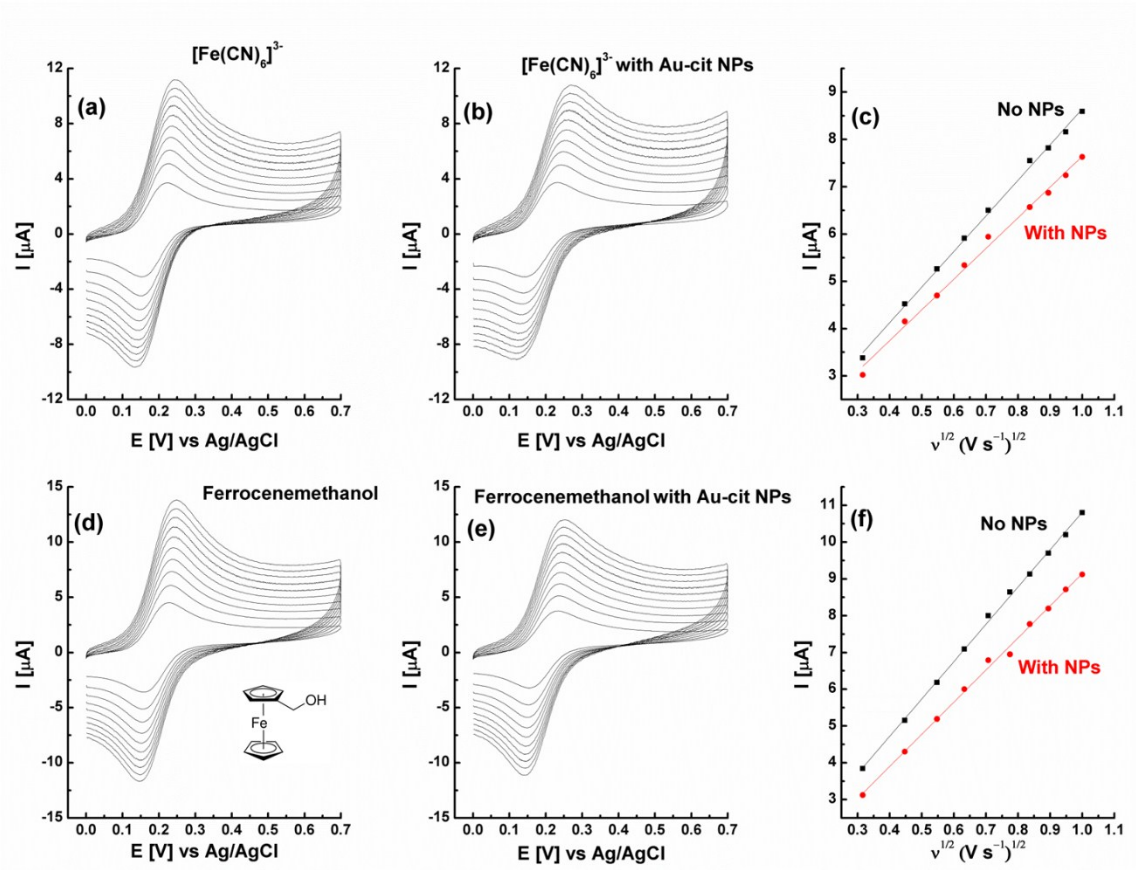

Figure S3: Cyclic voltammograms obtained at a GC electrode recorded at 0.1 to 1 V s^{-1} in 1 mM $K_3[Fe(CN)_6]$ and 0.1 M KNO_3 in the absence (a) and presence (b) of 50 pM Au-cit nanoparticles, (c) plot of peak current versus $v^{1/2}$ for the data shown in (a) and (b); and in 1 mM ferrocenemethanol and 0.1 M KNO_3 in the absence (d) and presence (e) of 50 pM Au-cit nanoparticles, (f) plot of peak current versus $v^{1/2}$ for the data shown in (d) and (e).

From the Randles-Sevcik analysis the diffusion coefficient of ferrocyanide was 2.5 x 10^{-6} cm^2 s^{-1} in the absence of NPs which decreased to 1.8 x 10^{-6} cm^2 s^{-1} in the presence of NPs. For ferrocenemethanol the diffusion coefficient was 4.6 x 10^{-6} cm^2 s^{-1} in the absence of NPs which decreased to 3.4 x 10^{-6} cm^2 s^{-1} in the presence of NPs.

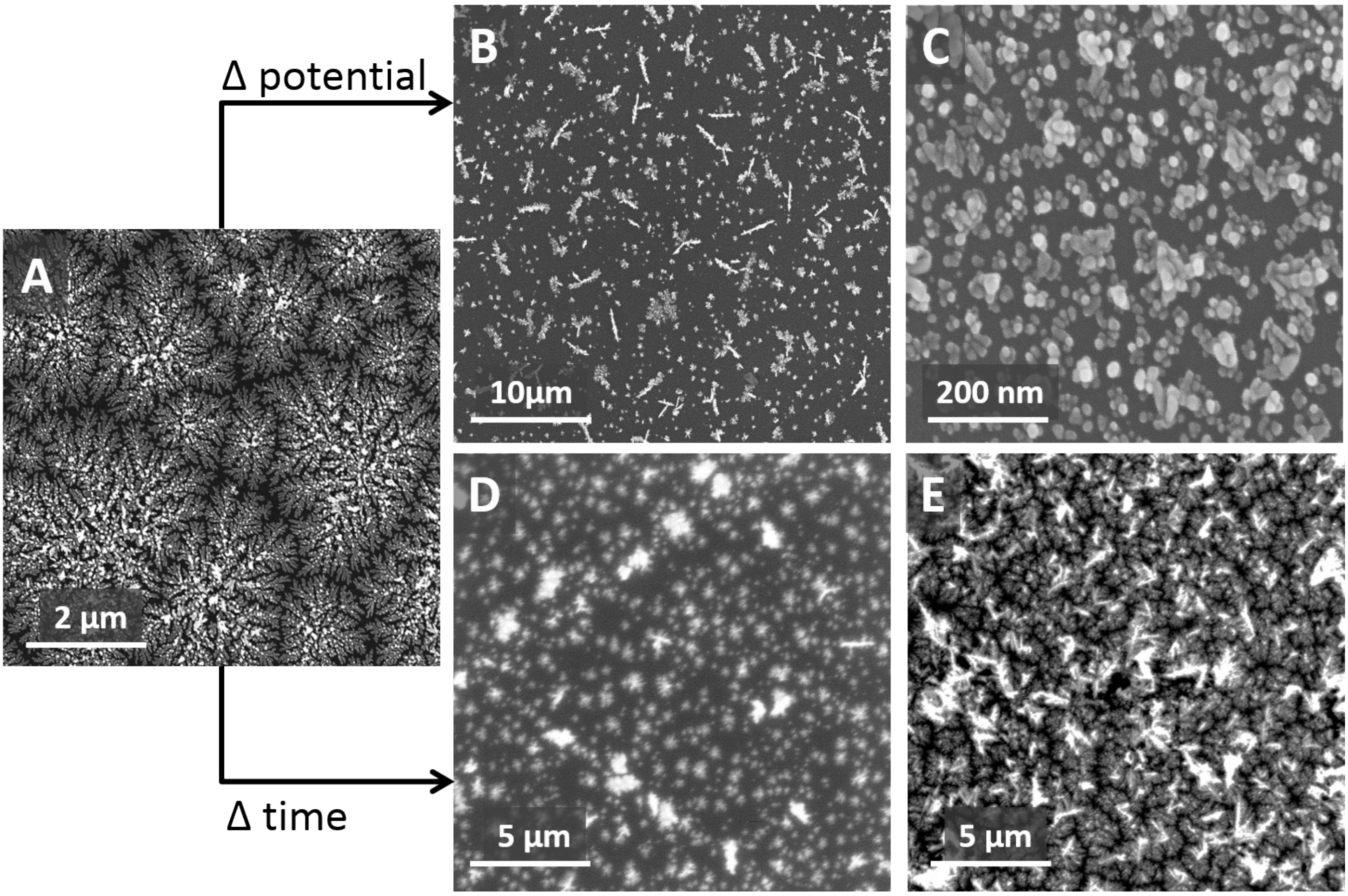

Figure S4: Scanning electron microscope images demonstrating the effect of potential and deposition time of Ag nanostructures electrodeposited in the presence of 500 µM Ag-tyr nanoparticles for 300 seconds at -100 mV (A), 100 mV (B) and -300 mV (C) and structures electrodeposited at -100 mV for 60 seconds (D) and 1000 seconds (E).

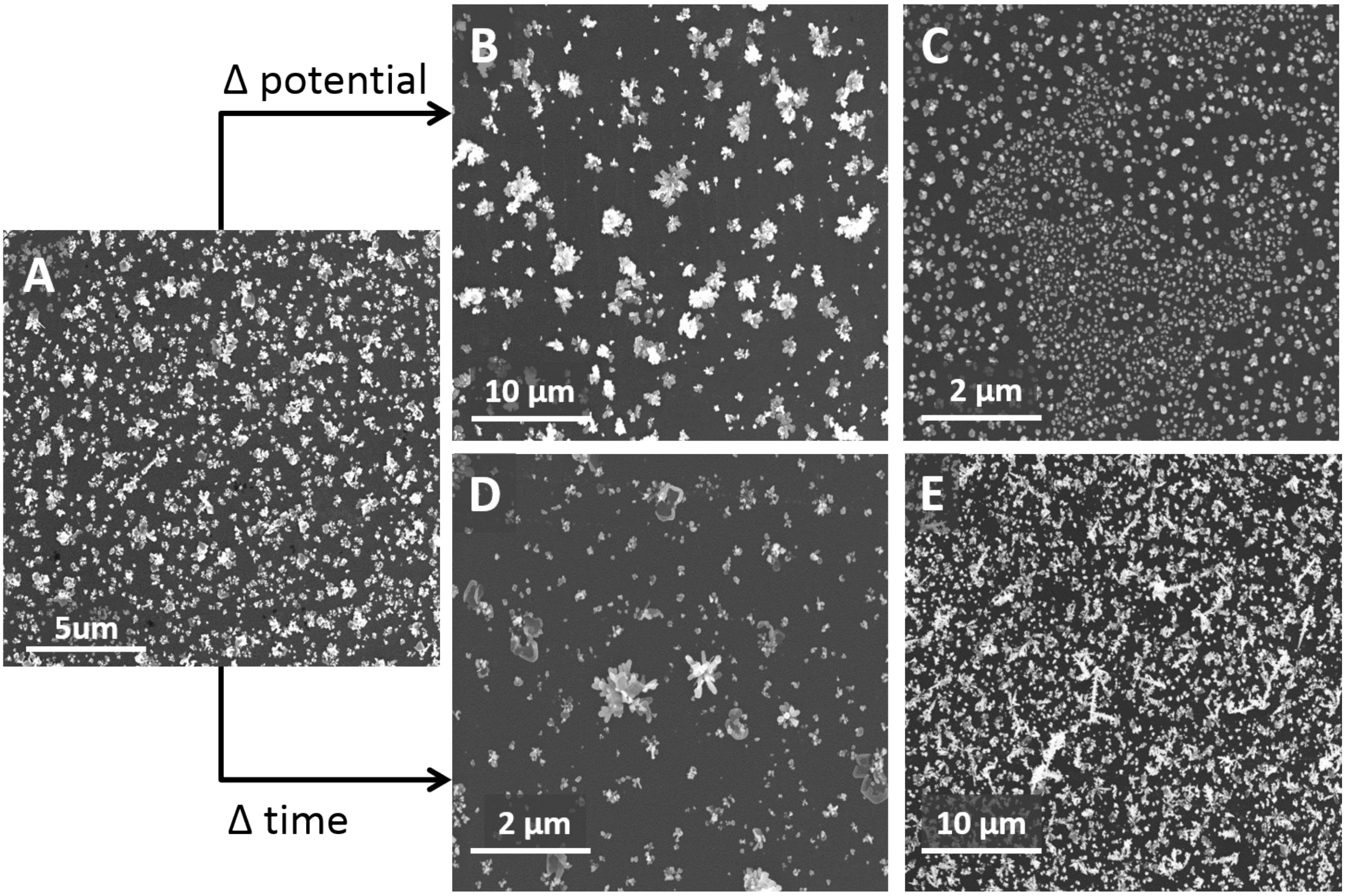

Figure S5: Scanning electron microscope images demonstrating a control study on the effect of potential and deposition time of Ag nanostructures electrodeposited in the **absence of any Ag-tyr nanoparticles** for 300 seconds at -100 mV (A), 100 mV (B) and -300 mV (C) and structures electrodeposited at -100 mV for 60 seconds (D) and 1000 seconds (E).

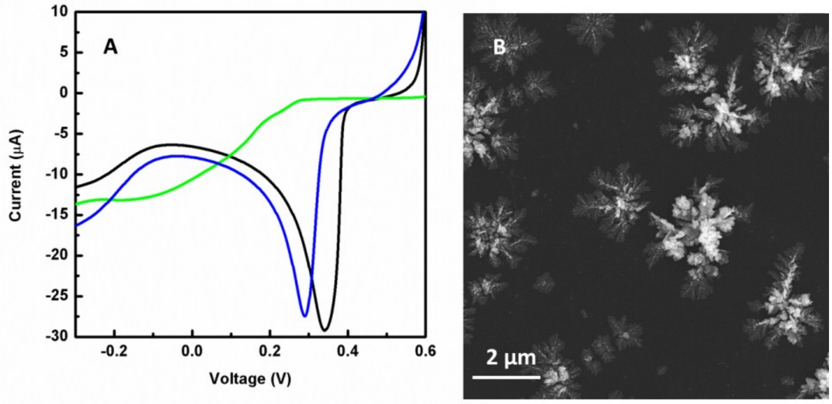

Figure S6: A) LSVs recorded at a GC electrode for the electrodeposition of Ag in an electrolyte containing 1 mM $AgNO_3$ (black), 1 mM $AgNO_3$ with 500 µM Ag NPs (blue) and 1 mM $AgNO_3$ and 0.5 mM tyrosine (green); B) SEM image of Ag electrodeposited at -100 mV for 300s on a GC electrode in 1 mM $AgNO_3$ containing 0.5 mM tyrosine.

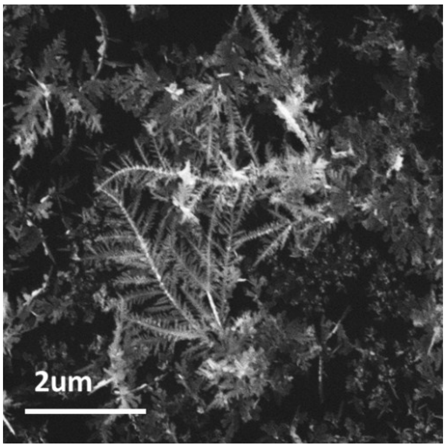

Figure S7: SEM image of Ag electrodeposited at -100 mV for 300s on a GC electrode in 1 mM $AgNO_3$ containing 50 µM of Au-cit NPs.

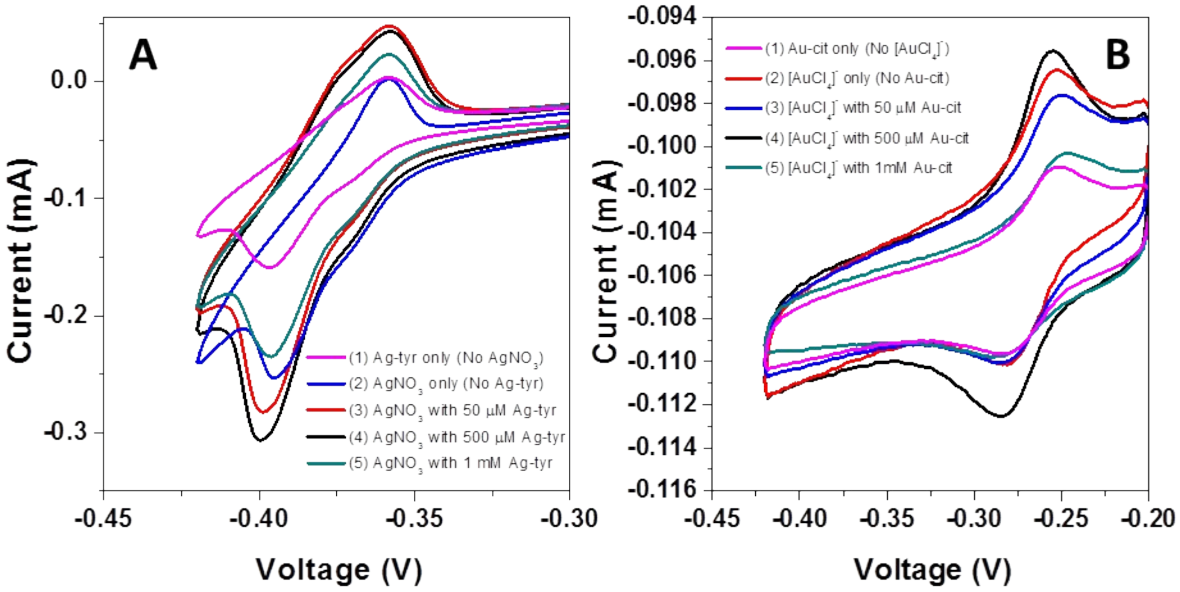

Figure S8: Pb underpotential deposition study, CVs obtained at a glassy carbon substrate with electrodeposited Ag (A) and Au (B) nanostructures at a sweep rate of 50 mV s^{-1} in 0.1 M HCl containing 10 mM $Pb(NO_3)_2$. The calculated surface area of the electrodeposited materials are detailed in the below table.

This was particularly important for the Ag system as calculating the area via analysis of the charge associated with oxide reduction is unreliable due to Ag dissolution.

Sample	Surface Area (cm^2)	Sample	Surface Area (cm^2)
Ag-tyr only	0.16	Au-cit only	0.30
$AgNO_3$ only	1.04	$[AuCl_4]^-$ only	1.40
$AgNO_3$ + 50µM Ag-tyr	2.1	$[AuCl_4]^-$ + 50µM Au-cit	1.76
$AgNO_3$ + 500µM Ag-tyr	2.05	$[AuCl_4]^-$ + 500µM Au-cit	1.73
$AgNO_3$ + 1mM Ag-tyr	0.98	$[AuCl_4]^-$ + 1mM Au-cit	1.13